Extracellular K^+ rapidly controls NaCl cotransporter phosphorylation in the native distal convoluted tubule by Cl^--dependent and independent mechanisms

Penton, David ; Czogalla, Jan ; Wengi, Agnieszka ; Himmerkus, Nina ; Loffing-Cueni, Dominique ; Carrel, Monique ; Rajaram, Renuga Devi ; Staub, Olivier ; Bleich, Markus ; Schweda, Frank ; Loffing, Johannes

Abstract: A high dietary potassium (K^+) intake causes a rapid dephosphorylation, and hence inactivation, of the thiazide-sensitive NaCl cotransporter (NCC) in the renal distal convoluted tubule (DCT). Based on experiments in heterologous expression systems, it was proposed that changes in extracellular K+ concentration ([K^+]ex) modulate NCC phosphorylation via a Cl^- -dependent modulation of the with no lysine (K) kinases (WNK)-STE20/SPS-1-44 related proline-alanine-rich protein kinase (SPAK)/oxidative stress-related kinase (OSR1) kinase pathway. We used the isolated perfused mouse kidney technique and ex vivo preparations of mouse kidney slices to test the physiological relevance of this model on native DCT. We demonstrate that NCC phosphorylation inversely correlates with [K^+]ex , with the most prominent effects occurring around physiological plasma [K^+]. Cellular Cl^- conductances and the kinases SPAK/OSR1 are involved in the phosphorylation of NCC under low [K^+]ex. However, NCC dephosphorylation triggered by high [K^+]ex is neither blocked by removing extracellular Cl^-, nor by the Cl^- channel blocker 4,4'-diisothiocyano-2,2'-stilbenedisulphonic acid. The response to [K^+]ex on a low extracellular chloride concentration is also independent of significant changes in SPAK/OSR1 phosphorylation. Thus, in the native DCT, [K^+]ex directly and rapidly controls NCC phosphorylation by Cl^--dependent and independent pathways that involve the kinases SPAK/OSR1 and a yet unidentified additional signalling mechanism.

DOI: https://doi.org/10.1113/JP272504

The Journal of Physiology

http://jp.msubmit.net

JP-RP-2016-272504R2

Title: Extracellular K^+ rapidly controls NCC phosphorylation in native DCT by Cl^--dependent and -independent mechanisms

Authors: David Penton
Jan Czogalla
Agnieszka Wengi
Nina Himmerkus
Dominique Loffing-Cueni
Monique Carrel
Renuga Rajaram
Olivier Staub
Markus Bleich
Frank Schweda
Johannes Loffing

Author Conflict: No competing interests declared

Author Contribution: David Penton: Conception and design; Collection and assembly of data; Data analysis and interpretation; Manuscript Writing; Final approval of manuscript (required) Jan Czogalla: Conception and design; Collection and assembly of data; Data analysis and interpretation; Manuscript Writing; Final approval of manuscript (required) Agnieszka Wengi: Collection and assembly of data; Data analysis and interpretation; Final approval of manuscript (required) Nina Himmerkus: Collection and assembly of data; Data analysis and interpretation; Final approval of manuscript (required) Dominique Loffing-Cueni: Collection and assembly of data; Data analysis and interpretation; Final approval of manuscript (required) Monique Carrel: Collection and assembly of data; Data analysis and interpretation; Final approval of manuscript (required) Renuga Rajaram: Collection and assembly of

data; Data analysis and interpretation; Final approval of manuscript (required) Olivier Staub: Conception and design; Data analysis and interpretation; Final approval of manuscript (required) Markus Bleich: Conception and design; Data analysis and interpretation; Final approval of manuscript (required) Frank Schweda: Conception and design; Data analysis and interpretation; Final approval of manuscript (required) Johannes Loffing: Conception and design; Financial Support; Collection and assembly of data; Data analysis and interpretation; Manuscript Writing; Final approval of manuscript (required)

Running Title: Mechanism of NCC regulation by K^+

Dual Publication: No

Funding: Swiss National Science Foundation (Schweizerische Nationalfonds): Johannes Loffing, 310030_143929/1; Swiss National Science Foundation (Schweizerische Nationalfonds): Olivier Staub, 310030_159765/1; NCCR Kidney.CH: Olivier Staub, Johannes Loffing; Cost Action Admire BM 13010: Olivier Staub, Johannes Loffing; DFG Sonderforschungsbereich 699: Frank Schweda; European Union 7th Framework: David Penton, 608847; HHS | National Institutes of Health (NIH): Nina Himmerkus, Markus Bleich, NIH R01DK084059

Extracellular K^+ rapidly controls NCC phosphorylation in native DCT by Cl^--dependent and -independent mechanisms

David Penton[1,5], Jan Czogalla[1,5], Agnieszka Wengi[1], Nina Himmerkus[2], Dominique Loffing-Cueni[1], Monique Carrel[1], Renuga Devi Rajaram[3,5], Olivier Staub[3,5], Markus Bleich[2], Frank Schweda[4], Johannes Loffing[1,5]

[1]Institute of Anatomy, University of Zurich, Switzerland, [2]Institute of Physiology, Christian-Albrecht University, Kiel, Germany. [3]Department of Pharmacology and Toxicology, University of Lausanne, Switzerland. [4]Institute of Physiology, University of Regensburg, Germany, [5]Swiss National Centre for Competence in Research "Kidney control of homeostasis"

DP and JC contributed equally to this work

Corresponding author*:*

Johannes Loffing
University of Zurich, Institute of Anatomy
Winterthurerstrasse 190, CH-8057 Zurich
Switzerland
Phone: +41 (0) 44 635 53 20
Fax: + 41 (0) 44 635 57 02
Email: johannes.loffing@anatom.uzh.ch

Running title*:*

Mechanism of NCC regulation by K^+

Keywords:

NaCl cotransporter, potassium, kidney

Key points summary:

- High dietary potassium (K^+) intake dephosphorylates and inactivates the NaCl cotransporter (NCC) in the renal distal convoluted tubule (DCT).
- Using several *ex-vivo* models, we show that physiological changes in extracellular K^+, like those occurring after a K^+ rich diet, are sufficient to promote a very rapid dephosphorylation of NCC in native DCT cells.
- Whilst the increase of NCC phosphorylation upon decreased extracellular K^+ appears to depend on cellular Cl^- fluxes, the rapid NCC dephosphorylation in response to increased extracellular K^+ is not Cl^- dependent.
- The Cl^- dependent pathway involves the SPAK/OSR1 kinases, whereas the Cl^- independent pathway may include additional signaling cascades.

Abstract

A high dietary potassium (K^+) intake causes a rapid dephosphorylation, and hence inactivation, of the thiazide-sensitive NaCl cotransporter (NCC) in the renal distal convoluted tubule (DCT). Based on experiments in heterologous expression systems, it was proposed that changes in extracellular K^+ concentration ($[K^+]_{ex}$) modulate NCC phosphorylation via a Cl^- dependent modulation of the WNK-SPAK/OSR1 kinase pathway. We used the isolated perfused mouse kidney technique and *ex vivo* preparations of mouse kidney slices to test the physiological relevance of this model on native DCT. We demonstrate that NCC phosphorylation inversely correlates with $[K^+]_{ex}$ with the most prominent effects occurring around physiological plasma $[K^+]$. Cellular Cl^- conductances and the kinases SPAK/OSR1 are involved in the phosphorylation of NCC under low $[K^+]_{ex}$. However, NCC dephosphorylation triggered by high $[K^+]_{ex}$ is neither blocked by removing extracellular Cl^-, nor by the Cl^- channel blocker DIDS. The response to $[K^+]_{ex}$ on low $[Cl^-]_{ex}$ is also independent from significant changes in SPAK/OSR1 phosphorylation. Thus, in the native DCT, $[K^+]_{ex}$ directly and rapidly controls NCC phosphorylation by Cl^- dependent and independent pathways that involve the kinases SPAK/OSR1 and yet unidentified additional signaling mechanism.

Abbreviations:

NCC, NaCl cotransporter; DCT, distal convoluted tubule; WNK, With no Lysine (K) kinases; SPAK, STE20/SPS-1- 44 related proline-alanine-rich protein kinase; OSR1, oxidative stress-related kinase, $[K^+]_{ex}$, extracellular potassium concentration; $[Cl^-]_{ex}$, extracellular chloride concentration; $[Cl^-]_i$, intracellular chloride concentration, PP, protein phosphatase; TAL, thick ascending limb of the Loop of Henle; IPK, isolated perfused mouse kidney; tNCC, total amount of NCC protein; pNCC, phosphorylated NCC in the position and amino acid indicated (ex pT53NCC: NCC phosphorylated in threonine 53); DIDS, 4,4'-Diisothiocyano-2,2'-stilbenedisulfonic acid; PP1 / PP2A, protein phosphatase 1 / 2A; PP3, protein phosphatase 3 or calcineurin.

Introduction

A high dietary potassium (K^+) intake has antihypertensive effects and improves cardiovascular outcomes (Mente *et al.*, 2014; O'Donnell *et al.*, 2014). These beneficial effects of a K^+ rich diet are likely related to a negative Na^+ balance due to an enhanced renal Na^+ excretion (Sorensen *et al.*, 2013; Mente *et al.*, 2014; Buendia *et al.*, 2015; Penton *et al.*, 2015). Indeed, oral K^+ loading promotes a rapid natriuresis that coincides with a dephosphorylation, and thus inactivation, of the thiazide-sensitive NaCl cotransporter (NCC) in the renal distal convoluted tubule (DCT) (Sorensen *et al.*, 2013). Conversely, dietary K^+ restriction increases NCC phosphorylation (Vallon *et al.*, 2009) and cell surface abundance of NCC (Frindt & Palmer, 2010), and also promotes a salt-sensitive rise in blood pressure (Vitzthum *et al.*, 2014) that depends on the presence of NCC (Terker *et al.*, 2015). Although an increase in NCC abundance was not always observed with dietary K^+ restriction (Nguyen *et al.*, 2012), the critical role of NCC for the maintenance of Na^+ homeostasis and the control of blood pressure is evidenced by the fact that thiazide diuretics are a mainstay of antihypertensive therapy. Furthermore, genetic diseases in which loss-of–function mutations in NCC and mutations in NCC-regulating kinases (With no Lysine (K) (WNK) WNK1 and WNK4) and ubiquitin-protein ligase complexes (KLHL3, cullin) cause hypotension and hypertension, respectively (Simon *et al.*, 1996; Wilson *et al.*, 2001).

The WNK kinases mediate their effects via phosphorylation of the STE20/SPS-1- 44 related proline-alanine-rich protein kinase (SPAK) and the related oxidative stress-related kinase (OSR1) which directly activate NCC by N-terminal phosphorylation (Hoorn *et al.*, 2011*a*). Based on studies in heterologous expression systems, it was proposed that the WNK and SPAK/OSR1 kinase pathway is critically involved in the

effect of dietary K^+ intake on NCC activity. In this model, altered dietary K^+ intake impacts on $[K^+]_{ex}$, which leads to changes in basolateral plasma membrane voltage and thus intracellular $[Cl^-]$ ($[Cl^-]_i$). Changes in $[Cl^-]_i$ have been shown to modulate the activities of both WNK1 (Piala *et al.*, 2014) and WNK4 (Bazúa-Valenti *et al.*, 2015) that ultimately regulate SPAK/OSR1 phosphorylation and activity, and thus NCC (Terker *et al.*, 2015). However, given the lack of an appropriate cell model that resembles the physiological complexity of native DCT cells, the relevance of this pathway for the DCT in the kidney *in vivo* is unclear. In fact, results from SPAK knock-out (Wade *et al.*, 2015), SPAK knock-in (Castañeda-Bueno *et al.*, 2014) and SPAK/OSR1 knock-out mouse models (Terker *et al.*, 2015) indicated that additional mechanisms must contribute as well. Moreover, the rapidity of NCC phosphorylation in response to an increased dietary K^+ load suggests that not only an inactivation of the phosphorylating kinase pathway, but also an activation of yet undefined dephosphorylating protein phosphatases, likely contributes towards the control of NCC phosphorylation by plasma $[K^+]$. Several protein phosphatases (PP) have been implicated in the modulation of NCC phosphorylation, including PP1 (Picard *et al.*, 2014), PP3 (calcineurin) (Lazelle *et al.*, 2016), and PP4 (Glover *et al.*, 2010). Nevertheless, to date no specific physiological function has been assigned to any of these phosphatases in the DCT.

Here we studied the response of native DCT cells to changes in $[K^+]_{ex}$ by combining *in vivo* and *ex vivo* methods. Our data support the hypothesis that the regulation of NCC phosphorylation triggered by changes in plasma K^+ occurs very rapidly and is mediated by Cl^- dependent and independent mechanism that involve SPAK/OSR1 and likely additional signaling pathways.

Methods

Ethical Approval

All animal experiments were conducted according to Swiss Laws and approved by the veterinary administration of the Canton of Zurich, Switzerland.

Reagents and antibodies

Unless otherwise stated, reagents were bought from Sigma Aldrich (Sigma, Buchs, Switzerland). DIDS and tacrolimus were purchased from Abcam (Abcam, Cambridge UK). Calyculin A was purchased from Cell Signaling Technologies (Massachusetts, USA). tNCC, pT53NCC, pT58NCC and pS71NCC antibodies were previously described (Wagner *et al.*, 2008; Sorensen *et al.*, 2013; Picard *et al.*, 2014). The pT96-pT101 NKCC2 antibody was generated by immunization of rabbits with a phospho-peptide (NH2-CLQ(pT)FGHN(pT)MD-CONH2) corresponding to the amino acids of mouse NKCC2 and subsequent affinity purification of the antibody (Pineda, Berlin, Germany). The specificity of the Ab towards pT96-pT101 NKCC2 was confirmed by immunohistochemistry. The antibody specifically stains the apical plasma membrane of the thick ascending limb. Pre-incubation of the antibody with the above mentioned phospho-peptide, but not with the corresponding dephospho-peptide abolished the immunostaining (data not shown). β-actin antibody was purchased from Sigma (Sigma, Buchs, Switzerland). Anti-Serine/threonine-protein Kinase 39 (labelled tSPAK in this manuscript) and anti-phospho-SPAK (Ser 373) / phospho-OSR1 (Ser 325) (labelled pSPAK-pOSR1 in this manuscript) antibodies were purchased from Millipore (Millipore, California USA).

Animals

Experiments were conducted in C57Bl/6 wildtype mice aged between 3 and 8 months. Mice were maintained at a 12/12 h light/dark cycle and had access to standard chow (3430, Provimi-Kliba, Switzerland) and water ad libitum. Animals were age, weight and gender matched for each experimental series.

KCl intravenous injections

Twelve hours before experiments, age and weight matched female animals were fasted, but free access to water was maintained. Animals were fixed in a supine position for surgery under anesthesia with isoflurane (Attane, Piramal, India). After median laparotomy, the vena cava was punctured using a 26G needle. Either 100 µl of 80 mmol/L KCl (in distilled H_2O with NaCl added to 300 mosmol/kg) or 0.9% NaCl as control were randomly injected. Either 5 or 15 minutes later, blood was withdrawn via the right ventricle. Blood was directly centrifuged, and the plasma collected and stored at -20°C for further analysis. Animals were then perfused with 20 ml ice-cold PBS via the abdominal aorta, kidneys removed, decapsulated, and snap frozen for western blot analysis.

Isolated perfused mouse kidney

Isolated mouse kidney perfusion was performed at 37°C in a small animal perfusion system (Hugo Sachs Elektronik, Germany) as previously described (Schweda *et al.*, 2003). Age and weight matched male animals were used. In all experiments, kidneys were first perfused for 30 minutes (pressure-fixed 90 mmHg) with buffer (see supplementary material for precise buffer composition) containing 4.5 mmol/L K^+. Afterwards, buffer [K^+] was randomly adapted by adding KCL to a K^+ concentration ranging between 3.2 and 10.38 mmol/L, and kidneys were perfused for a further 30

minutes. After 1 hour, perfusion was stopped and kidneys were snap frozen in liquid nitrogen for western blot analysis. NCC phosphorylation in perfused kidneys was normalized to NCC phosphorylation in contralateral kidneys from same animals, which were removed and snap frozen at the beginning of the procedure. For immunohistochemistry studies, after perfusion with either 4.5 or 10 mmol/L [K^+] for one hour, 3% PFA was added to the perfusion buffer. 50 mL of buffer + fixative were infused at 200 mmHg and washed out with 50ml buffer without fixative at 120 mmHg. The kidneys were post-fixed in 1.5% PFA at 4°C overnight and processed as described previously for immunofluorescence microscopy (Sorensen *et al.*, 2013).

Kidney slices preparation

Gender, age, and weight matched mice were used for kidney slices preparation. Both kidneys were quickly removed under deep isoflurane anesthesia (Attane, Piramal, India) and 280 µm thick slices were cut with a vibrating microslicer (Vibratome, Microm). Slicing was performed in ice-cold Ringer-type solution (in mmol/L): 98.5 NaCl, 35 $NaHCO_3$, 3 KCl, 1 NaH_2PO_4, 2.5 $CaCl_2$, 1.8 $MgCl_2$, 25 Glucose. The slices were incubated for equilibration in a similar Ringer-type solution (25 mmol/L $NaHCO_3$) for 30 minutes at 30,5°C. Afterwards, the slices were transferred to the incubation chambers containing the effector or control solutions. All solutions were continuously bubbled with 95% O_2 and 5% CO_2. In experiments in which $[K^+]_{ex}$ was changed, osmolarity and $[Cl^-]_{ex}$ were kept constant by addition of equal amounts of NaCl (or Na-Gluconate in low $[Cl^-]_{ex}$ experiments). Some slices exposed to varying $[K^+]_{ex}$, were incubated also in the presence isoproterenol (100 nmol/L) or calyculin A (20 nmol/L) dissolved in DMSO, or tacrolimus (10 µmol/L) dissolved in ethanol. In parallel, slices were incubated with either DMSO or ethanol in the appropriate amount and used as control vehicle. After 30 minutes incubation

with the effectors, slices were snap frozen in liquid nitrogen and processed for immunoblotting.

Reversibility of NCC dephosphorylation

After equilibration under control conditions (3 mmol/L $[K^+]_{ex}$) for 30 minutes, kidney slices were transferred to incubation chambers containing either 1, 3 or 10 mmol/L $[K^+]_{ex}$ (low, control, high $[K^+]_{ex}$ respectively) and incubated for another 30 minutes, as described before. Next, slices previously incubated with 10 mmol/L $[K^+]_{ex}$ were transferred to the 1 mmol/L $[K^+]_{ex}$ chamber and incubated for a further 30 minutes. After 90 minutes total incubation time, slices from each incubation condition were collected and processed for immunoblotting.

DCT microperfusion

DCTs were morphologically identified and isolated manually from kidney slices after enzymatically assisted separation of nephron segments using a dissection microscope, as previously described (Pohl *et al.*, 2010; Gong *et al.*, 2015). The preparation solution contained (in mmol/L): 49 NaCl, 3 KCl, 0.4 NaH_2PO_4, 1.6 Na_2HPO_4, 1 $MgCl_2$, 2.3 Ca-gluconate, 190 mannitol, 5 glucose. 10 DCTs per condition were microperfused using a double-barrelled perfusion pipette, as described previously (Greger, 1981) with a solution containing (in mmol/L): 50 NaCl, 2 KCl, 0.4 NaH_2PO_4, 1.6 Na_2HPO_4, 1 $MgCl_2$, 2.3 Ca-gluconate, 190 mannitol, 5 glucose for 10 minutes at 37 °C. The basolateral solution contained (in mmol/L): 105 NaCl, 0.4 NaH_2PO_4, 1.6 Na_2HPO_4, 1 $MgCl_2$, 2.3 Ca-gluconate, 30 Na-gluconate, 5 glucose. KCl (1, or 10 mmol/L) was added depending on the experimental condition and the osmolarity of the solutions was equilibrated with NaCl accordingly. Following perfusion, DCTs were collected from the chamber, pooled, and processed for

immunoblotting. In addition samples of 10-15 unperfused DCTs were incubated in preparation solution for 10 minutes at 37°C.

Aldosterone measurements

For aldosterone measurements, 10 µL of plasma was diluted in 40 µl of 0.9% NaCl and measured in triplicates using an Aldosterone ELISA Kit (CAN-ALD-450, Diagnostics Biochem Canada Inc., Canada) and a Tecan plate reader (Tecan infinite F200 pro, Tecan Group AG, Switzerland) according to manufacturer's instructions.

Plasma electrolyte analysis

Plasma electrolyte levels were measured in 100 µL of undiluted plasma using an EFOX 5053 flame photometer (Eppendorf, Eppendorf, Germany).

Immunoblotting

Kidney samples were homogenized in a Precellys 24 homogenizer or by ultrasound in lysis buffer containing protease inhibitor cocktail (Complete, Roche Diagnostics), phosphatase inhibitor (Phosstop, Roche Diagnostics), and (in mmol/L) 200 Mannitol, 80 Hepes, 41 KOH (pH corrected to 7.4). Homogenized samples without any further manipulation, or the supernatant from the samples centrifuged for 10 minutes 4.000 x g at 4°C (whole animal studies or isolated perfused kidney), were then used for western blotting. Protein concentration was assessed via Bradford assay (CooAssay Protein Dosage Reagent, Uptima, France). 25 µg (or 50 µg for the detection of SPAK and pSPAK-pOSR1) of protein was solubilized in loading buffer (31.5 mmol/L Tris-HCl, 1% SDS, 0.005% Bromphenol blue, 12.5% glycerol and 5% ß-mercaptoethanol, pH 6.5), run in an 8% SDS PAGE and transferred to nitrocellulose membranes. Membranes were blocked for 20 minutes in blocking buffer (Odyssey blocking buffer,

Li-Cor Biosciences, USA) and incubated with primary antibodies at 4°C overnight. Membranes were further incubated for 2 hours at room temperature with the appropriate secondary antibodies and imaged using a Li-Cor infrared scanner (Li-Cor Biosciences, USA). Optical density of bands was quantified using ImageJ software (http://imagej.nih.gov/ij/) and normalized to the corresponding band densities in a coomassie-stained gel (ProtoBlue Safe, National Diagnostics, UK) that was loaded and run in parallel. A protein dilution series was performed for each antibody and confirmed that signal detection and analysis were performed in the linear range of the system. Detection of β-actin was used to visualize equal loading.

Statistics

Unpaired Student's t-test was used to compare between two groups. For multiple comparison, one way ANOVA with Bonferroni's multiple comparison post-test was performed using the software OriginPro 2015 (OriginLab Corporation, Massachusetts, USA).

Results

Small variations of plasma [K^+] rapidly modulate NCC phosphorylation

In previous experiments in mice, we found that oral K^+ loading rapidly increases plasma [K^+] and dephosphorylates NCC (Sorensen *et al.*, 2013). Likewise, further analysis of rat and mouse models suggested an inverse correlation between plasma [K^+] and NCC phosphorylation (Rengarajan *et al.*, 2014; Terker *et al.*, 2016). To test experimentally whether altered plasma [K^+] could directly account for the observed rapid changes of NCC phosphorylation in the kidney we performed two types of experiments. Firstly, we injected intravenously 100 µl of either vehicle or 80 mmol/L KCl in mice. The KCl injection increased plasma [K^+] significantly (Fig 1A) while the plasma concentrations of Na^+ and aldosterone remained largely unchanged within the time frame analyzed (Fig 1B and C). NCC phosphorylation at all tested sites (T53, T58 and S71) was decreased 5 minutes after KCl injection; the effect was even more pronounced at 15 minutes (Fig 1D). Next, we perfused isolated mouse kidneys *ex vivo* with buffers containing different concentrations of K^+ ranging from 3.2 to 10.38 mmol/L. To counterbalance the inter-individual variation, NCC phosphorylation in the perfused kidney was normalized to NCC phosphorylation in the intact contralateral kidney from the same animal (Fig 1E). We observed a clear inverse dose-response relationship between [K^+] and NCC phosphorylation (Fig 1F and supplementary material) with the most pronounced changes in NCC phosphorylation occurring between 3 and 5 mmol/L of [K^+]. Consistent with previous *in vivo* data (Sorensen *et al.*, 2013; Rengarajan *et al.*, 2014; Terker *et al.*, 2015), the effect of K^+ on the isolated perfused kidney *ex vivo* was specific for NCC since the phosphorylation of the closely related transporter NKCC2 in the thick ascending limb of the Loop of Henle (TAL) remained stable, regardless of [K^+] (Fig 1G).

The kidney slice model reproduces the *in vivo* findings

The isolated perfused mouse kidney (IPK) model allowed us to assess the effect of K^+ on the DCT in an intact organ whilst simultaneously avoiding systemic effects of confounding factors such as hormones and renal innervation. Nevertheless, with this system we could not exclude the influence of changes in tubular flow and intrarenal hemodynamics on DCT function. Given the lack of an appropriate DCT cell model suitable to assess the direct effect of $[K^+]$, we used simple kidney slice preparations to study *ex vivo* acute changes in NCC phosphorylation in native DCT cells. First we studied the behavior of tNCC and pNCC in kidney slices incubated with control Ringer-type buffer (3 mmol/L $[K^+]_{ex}$) during the course of one hour. Under these conditions, the abundance of tNCC remained stable between 15 and 60 minutes of incubation, while pT53NCC decreased continuously with time (Fig 2A and 2B). As we observed a stable NCC phosphorylation between 30 and 60 minutes of incubation, all further experiments were performed during this time frame, unless stated otherwise.

First, we analyzed the effect of elevated $[K^+]_{ex}$. While $[K^+]$ did not affect tNCC, the drop in pT53NCC over time was steeper in slices incubated with 10 mmol/L $[K^+]_{ex}$ as compared to those incubated in 3 mmol/L $[K^+]_{ex}$ buffer (Fig 2C and 2D).

NCC phosphorylation is modified by manipulations that affect DCT membrane voltage.

The membrane voltage of DCT cells is supposed to be controlled by the activity of the basolateral K^+ channel $Kir_{4.1}$ (KCNJ10 gene) (Reichold *et al.*, 2010; Zhang *et al.*, 2014) which functions as heterotetramer with $Kir_{5.1}$ (KCNJ16). Under physiological conditions, KCNJ10/16 is believed to hyperpolarize DCT basolateral plasma

membrane voltage (Paulais *et al.*, 2011). Thus, increasing $[K^+]_{ex}$ should depolarize DCT cells, while hyperpolarization will occur under low $[K^+]_{ex}$. We addressed the question whether manipulations promoting changes in the membrane voltage of DCT cells were sufficient to modulate NCC phosphorylation. The phosphorylation of NCC was assessed by immunoblotting after incubating kidney slices for 30 minutes with different $[K^+]_{ex}$. While tNCC remained stable under all $[K^+]_{ex}$ investigated (fig 3A and 3B), pT53NCC showed an inverse dose response curve in response to changes in $[K^+]_{ex}$ (Fig 3A and 3C). In agreement with the results obtained *in vivo* and with the IPK model, physiologically relevant variations in $[K^+]_{ex}$ were already sufficient to induce statistically significant changes in NCC phosphorylation ($[K^+]_{ex}$ 3 mmol/L =100 ± 4.7 % of pT53NCC; $[K^+]_{ex}$ 5 mmol/L =56.0 ± 7.0 % of pT53NCC; $p<0.001$). Furthermore, NCC dephosphorylation could be partially reversed by transferring the slices from high $[K^+]_{ex}$ (10 mmol/L) to low $[K^+]_{ex}$ (1mmol/L) (Fig 3D). Moreover, the addition of the potassium channel blocker $BaCl_2$ (5 mmol /L) was sufficient to promote the dephosphorylation of NCC (Fig 3E and 3F).

DCTs express K^+ channels on both the apical and the basolateral membrane (Bandulik *et al.*, 2011), and these channels could potentially sense changes in K^+ intake. To assess whether changes of $[K^+]_{ex}$ on the basolateral (blood) side are sufficient to promote changes in NCC phosphorylation, DCTs were isolated by hand and exposed at the basolateral cell side to either 1 or 10 mmol/L $[K^+]_{ex}$. The lumen was microperfused with 2 mmol/L K^+ and 50 mmol/L Na^+, which recapitulates the physiological luminal K^+ and Na^+ concentrations as previously observed by *in vivo* micropuncture measurements (Weinstein, 2012). Subsequently, changes in the phosphorylation of NCC were assessed by immunoblotting. As evident in figure 3G, lowering basolateral $[K^+]_{ex}$ to 1 mmol/L triggered the phosphorylation of NCC within

10 minutes; at 10 mmol/L of basolateral $[K^+]_{ex}$, the phosphorylation of NCC was almost completely abolished.

Low $[Cl^-]_{ex}$ clamps SPAK/OSR1 phosphorylation but does not prevent NCC dephosphorylation in response to high $[K^+]_{ex}$

Changes in intracellular $[Cl^-]_i$ have been proposed to underlie the modifications of NCC phosphorylation in response to altered $[K^+]_{ex}$ (Zhang *et al.*, 2014; Terker *et al.*, 2015). According to this hypothesis, $[K^+]_{ex}$ affects membrane voltage, which changes the driving force for Cl^- to exit the cell through chloride channels in the basolateral membrane of DCT cells. Thus, a hyperpolarized cell membrane will lead to an increased Cl^- exit, therefore lowering its intracellular concentration; on the contrary, depolarized cells will retain Cl^-. These secondary changes in $[Cl^-]_i$ were proposed to regulate the phosphorylation of SPAK and NCC, due to the inhibitory effect of $[Cl^-]_i$ on WNK1 and WNK4 (Alessi *et al.*, 2014). Indeed, increasing $[K^+]_{ex}$ promotes both NCC and SPAK/OSR1 dephosphorylation (Fig 4A, 4C and 4D).

To test the hypothesis that cellular Cl^- fluxes and altered SPAK activity contribute to the regulation of NCC by $[K^+]_{ex}$, we compared kidneys slices incubated with either a standard buffer (110 mM $[Cl^-]_{ex}$) or a buffer in which almost all Cl^- was replaced by using sodium gluconate instead of NaCl (5 mM $[Cl^-]_{ex}$). Under standard conditions ($[Cl^-]_{ex}$ 110 mM), lowering $[K^+]_{ex}$ increased SPAK/OSR1 and NCC phosphorylation while high $[K^+]_{ex}$ had opposing effects (Fig 4A, 4C and 4D). Lowering $[Cl^-]_{ex}$ to 5 mmol/L significantly increased NCC phosphorylation (Fig 4C). Under this low $[Cl^-]_{ex}$ condition, we did not see any increase in either SPAK/OSR1 or NCC phosphorylation in response to lowering $[K^+]_{ex}$ from 3 (control) to 1 (low) mmol/L (Fig 4B, 4C and 4D). Nevertheless, NCC phosphorylation on low $[Cl^-]_{ex}$ condition could still be enhanced by isoproterenol , which was previously described as an activator

of NCC phosphorylation (Terker *et al.*, 2014) (Fig 4 G). This indicates that the lack of response to low $[K^+]_{ex}$ is not explained by an already maximal stimulation of NCC. In contrast to the diminished response to low $[K^+]_{ex}$, NCC was still dephosphorylated when $[K^+]_{ex}$ was increased from 3 (control) to 10 (high) mmol/L (Fig 4B and 4C). The extent of the dephosphorylation was comparable to the one at baseline $[Cl^-]_{ex}$ (80.9 ± 11.8% vs 72.5 ± 19.0%; under 110 vs 5 mmol/L $[Cl^-]_{ex}$, respectively). Interestingly, the dephosphorylation of NCC occurred independently from any significant change in SPAK/OSR1 phosphorylation, which remained clamped at a high level (Fig 4B and 4D). Consistent with the Cl^- replacement studies, inhibition of plasma membrane Cl^- fluxes with the Cl^- channel blocker 4,4'-Diisothiocyano-2,2'-stilbenedisulfonic acid (DIDS) (0.5 mmol/L) did not prevent NCC dephosphorylation in response to increasing $[K^+]_{ex}$ from 3 (control) to 10 (high) mmol/L (Fig 4E and 4F).

High $[K^+]_{ex}$ induced dephosphorylation of NCC is not blocked by inhibition of protein phosphatase 1, 2A and 3

Given the evidence described above for SPAK-independent effects of $[K^+]_{ex}$ on NCC, and also the rapid kinetics of NCC dephosphorylation, we tested whether some of the known NCC regulating protein phosphatases might be involved in mediating the effect of high $[K^+]_{ex}$ on NCC. Incubation of tissue slices with neither the protein phosphatase 1 and 2A inhibitor calyculin A (Sorensen *et al.*, 2013), nor with the protein phosphatase 3 (calcineurin) inhibitor tacrolimus (Hoorn *et al.*, 2011*b*) prevented the dephosphorylation of NCC in response to increased $[K^+]_{ex}$ on standard $[Cl^-]_{ex}$ (Fig 5A-5C).

Discussion

Dietary K^+ intake has a strong impact on the phosphorylation, and hence activity, of NCC in the DCT. Previous studies have correlated these effects to altered plasma K^+ levels and suggested a model in which the extracellular K^+ concentration, via altered membrane voltage and intracellular Cl^- concentrations, regulates the WNK- and SPAK-dependent phosphorylation of NCC. In the present study, we employed three different *ex vivo* models (i.e. the isolated perfused kidney, the isolated perfused tubule and kidney slices) to experimentally test this hypothesis on the native DCT. Our data provide clear evidence for rapid and direct effects of $[K^+]_{ex}$ on NCC phosphorylation and suggest that aside from the WNK/SPAK kinase pathway also the protein phosphatase 3 (calcineurin) additionally contributes to the regulation of NCC by $[K^+]_{ex}$.

Rengarajan and co-workers showed that 3 hours intravenous infusion of KCl reduces phosphorylation of NCC and marginally of SPAK in parallel to increased plasma $[K^+]$ (Rengarajan *et al.*, 2014). Likewise, Terker *et al.* described for various mouse models a clear inverse relationship between plasma $[K^+]$ and NCC phosphorylation suggesting that plasma $[K^+]$ may have direct effects on the native DCT (Terker *et al.*, 2016). However, these data were correlative and did not allow for clear cause-effect conclusions. The possible regulatory effect of humoral kaliuretic factors and/or nerval reflexes (Rabinowitz, 1996) could not be excluded. Now, by using three independent *ex vivo* approaches, we provide consistent and conclusive evidence that $[K^+]_{ex}$ directly modulates NCC phosphorylation in native DCT cells. This regulation occurs very rapidly (<30 minutes) and is particularly prominent in the range of physiological plasma $[K^+]$, suggesting that transient and small variations in plasma (K^+), as they may occur in response to a meal, may already be sufficient to modulate NCC activity

and hence renal Na^+ reabsorption. However, the present *ex vivo* data contrast with our previous data on isolated DCT preparations in which we failed to observe any significant NCC dephosphorylation after increasing extracellular K^+ from 5 to 10 mmol/L (Sorensen *et al.*, 2013). As we demonstrate in the present study, 5 mmol/L is already on the upper $[K^+]$ limit rendering almost all NCC dephosphorylated. Nevertheless, DCTs are still able to respond to decreased $[K^+]_{ex}$, as demonstrated by the isolated perfused DCT technique.

Based on experiments using whole animal and heterologous expression system models, Terker and co-workers recently hypothesized that DCT cells depolarize upon an increase in plasma $[K^+]$. The subsequent increase in $[Cl^-]_i$ leads to decreased phosphorylation of NCC via the inhibition of the WNK-SPAK/OSR1 kinase pathway (Terker *et al.*, 2015). In agreement with this hypothesis, we found in native DCTs that both an increase of $[K^+]_{ex}$ and the addition of the K^+ channel blocker $BaCl_2$ to the incubation buffer triggered a pronounced dephosphorylation of NCC. In contrast, removal of extracellular Cl^-, which presumably lowers intracellular Cl^-, significantly increased NCC phosphorylation, and blocked the stimulatory effect of low $[K^+]_{ex}$ on NCC. However, although these data are suggestive for an involvement of plasma membrane voltage and intracellular $[Cl^-]$, we could not directly analyze these parameters in our *ex vivo* preparations for technical reasons, including an insufficient up-take of Cl^--sensitive dyes into DCT cells. Other mechanisms, such as changes in cell volume, remain to be considered. Indeed, hypo-osmotic cell swelling stimulates SPAK-dependent NCC activation (Richardson *et al.*, 2008) and recent data suggest that WNK4 is phosphorylated in response to osmotic stress (Maruyama *et al.*, 2016).

Interestingly, when we reduced $[Cl^-]_{ex}$ to very low levels, thereby clamping SPAK-OSR1 phosphorylation to very high levels, only the response of NCC to low $[K^+]_{ex}$, not high $[K^+]_{ex}$, was blocked. Likewise, blocking Cl^- channels with DIDS did not prevent the dephosphorylation of NCC under high $[K^+]_{ex}$, suggesting that additional mechanisms to the proposed pathway via Cl^- dependent changes in WNK-SPAK/OSR1 activity are also involved in the regulation of NCC phosphorylation by K^+. It was already evident from the data provided by Terker and coworkers (Terker *et al.*, 2015) that the SPAK/OSR1 single and double knockout mice were still able to modulate NCC phosphorylation to some extent in response to low dietary K^+ intake. Moreover, Castañeda-Bueno and coworkers reported changes in NCC and its phosphorylation in response to changes in dietary K^+ in WNK4 knockout mice (Castañeda-Bueno *et al.*, 2014). Furthermore, Wade and coworkers reported an increase in NCC phosphorylation in response to low K^+ diet in SPAK knockout mice (Wade *et al.*, 2015).

The rapidity of NCC phosphorylation in response to K^+ infusion, already evident within 5 minutes, suggests that in addition to a shut-down of NCC phosphorylation by kinases, an activation of NCC dephosphorylation via phosphatases may also contribute to the observed effects. Previous studies had implicated various phosphatases in the control of NCC function (Glover *et al.*, 2010; Hoorn *et al.*, 2011*b*; Picard *et al.*, 2014). PP1 and PP3 are highly abundant in the DCT and inhibition of PP1 and PP3 by calyculin A and tacrolimus, respectively, increases NCC phosphorylation (Hoorn *et al.*, 2011*b*; Picard *et al.*, 2014). PP3 inhibition does also likely explain NCC-dependent salt-sensitive hypertension in patients under immunosuppressive therapy with calcineurin inhibitors (Hoorn *et al.*, 2011*b*; Borschewski *et al.*, 2016). Likewise, a kidney-specific deletion of FK506 binding

protein, crucial for the effects of tacrolimus on PP3, attenuates tacrolimus-induced arterial hypertension (Lazelle *et al.*, 2016). However, in our experiments inhibition of PP1 and PP3 did not block the $[K^+]_{ex}$-induced dephosphorylation of NCC, suggesting that other signaling cascades are involved.

In conclusion, we showed that $[K^+]_{ex}$ directly controls NCC phosphorylation in native DCT cells. The effect of low $[K^+]_{ex}$ on NCC likely involves altered transmembrane Cl^- fluxes and an activation of SPAK/OSR1, while the rapid effects of high $[K^+]_{ex}$ do not critically depend upon transmembrane Cl^- permeability and may include both an inhibition of SPAK/OSR1 and the activation of yet not identified signaling pathways. Based on the rapidity of NCC dephosphorylation in response to $[K^+]_{ex}$, we hypothesize that protein phosphatases are involved. Our data, might stimulate further research to identify these additional mechanism.

References

Alessi DR, Zhang J, Khanna A, Hochdörfer T, Shang Y & Kahle KT (2014). The WNK-SPAK/OSR1 pathway: master regulator of cation-chloride cotransporters. *Sci Signal* **7,** re3.

Bandulik S, Schmidt K, Bockenhauer D, Zdebik A a, Humberg E, Kleta R, Warth R & Reichold M (2011). The salt-wasting phenotype of EAST syndrome, a disease with multifaceted symptoms linked to the KCNJ10 K+ channel. *Pflugers Arch* **461,** 423–435.

Bazúa-Valenti S, Chávez-Canales M, Rojas-Vega L, González-Rodríguez X, Vázquez N, Rodríguez-Gama A, Argaiz ER, Melo Z, Plata C, Ellison DH, García-Valdés J, Hadchouel J & Gamba G (2015). The Effect of WNK4 on the Na+-Cl- Cotransporter Is Modulated by Intracellular Chloride. *J Am Soc Nephrol* **26,** 1781–1786.

Borschewski A, Himmerkus N, Boldt C, Blankenstein KI, McCormick J a, Lazelle R, Willnow TE, Jankowski V, Plain A, Bleich M, Ellison DH, Bachmann S & Mutig K (2016). Calcineurin and Sorting-Related Receptor with A-Type Repeats Interact to Regulate the Renal Na^+-K^+-$2Cl^-$ Cotransporter. *J Am Soc Nephrol* **27,** 107–119.

Buendia JR, Bradlee ML, Daniels SR, Singer MR & Moore LL (2015). Longitudinal Effects of Dietary Sodium and Potassium on Blood Pressure in Adolescent Girls. *JAMA Pediatr* **02118,** 1–9.

Castañeda-Bueno M, Cervantes-Perez LG, Rojas-Vega L, Arroyo-Garza I, Vázquez N, Moreno E & Gamba G (2014). Modulation of NCC activity by low and high K(+) intake: insights into the signaling pathways involved. *Am J Physiol Renal Physiol* **306,** F1507–F1519.

Frindt G & Palmer LG (2010). Effects of dietary K on cell-surface expression of renal ion channels and transporters. *Am J Physiol Renal Physiol* **299,** F890–F897.

Glover M, Mercier Zuber A, Figg N & O'Shaughnessy KM (2010). The activity of the thiazide-sensitive Na(+)-Cl(-) cotransporter is regulated by protein phosphatase PP4. *Can J Physiol Pharmacol* **88,** 986–995.

Gong Y, Himmerkus N, Plain A, Bleich M & Hou J (2015). Epigenetic regulation of microRNAs controlling CLDN14 expression as a mechanism for renal calcium handling. *J Am Soc Nephrol* **26,** 663–676.

Greger R (1981). Cation selectivity of the isolated perfused cortical thick ascending limb of Henle's loop of rabbit kidney. *Pflügers Arch Eur J Physiol* **390,** 30–37.

Hoorn EJ, Nelson JH, McCormick J a & Ellison DH (2011*a*). The WNK Kinase Network Regulating Sodium, Potassium, and Blood Pressure. *J Am Soc Nephrol* **22,** 605–614.

Hoorn EJ, Walsh SB, McCormick JA, Fürstenberg A, Yang C-L, Roeschel T, Paliege A, Howie AJ, Conley J, Bachmann S, Unwin RJ & Ellison DH (2011*b*). The calcineurin inhibitor tacrolimus activates the renal sodium chloride cotransporter to cause hypertension. *Nat Med* **17,** 1304–1309.

Lazelle R a., McCully BH, Terker AS, Himmerkus N, Blankenstein KI, Mutig K, Bleich M, Bachmann S, Yang C-L & Ellison DH (2016). Renal Deletion of 12 kDa FK506-Binding Protein Attenuates Tacrolimus-Induced Hypertension. *J Am Soc Nephrol* **27,** 1456–1464.

Maruyama J, Kobayashi Y, Umeda T, Vandewalle A, Takeda K, Ichijo H & Naguro I (2016). Osmotic stress induces the phosphorylation of WNK4 Ser575 via the p38MAPK-MK pathway. *Sci Rep* **6,** 18710.

Mente A et al. (2014). Association of urinary sodium and potassium excretion with blood pressure. *N Engl J Med* **371,** 601–611.

Nguyen MTX, Yang LE, Fletcher NK, Lee DH, Kocinsky H, Bachmann S, Delpire E & McDonough A a (2012). Effects of K+-deficient diets with and without NaCl supplementation on Na+, K+, and H2O transporters' abundance along the nephron. *Am J Physiol Renal Physiol* **303,** F92–F104.

O'Donnell M et al. (2014). Urinary Sodium and Potassium Excretion, Mortality, and Cardiovascular Events. *N Engl J Med* **371,** 612–623.

Paulais M, Bloch-Faure M, Picard N, Jacques T, Ramakrishnan SK, Keck M, Sohet F, Eladari D, Houillier P, Lourdel S, Teulon J & Tucker SJ (2011). Renal phenotype in mice lacking the Kir5.1 (Kcnj16) K+ channel subunit contrasts with that observed in SeSAME/EAST syndrome. *Proc Natl Acad Sci U S A* **108,** 10361–10366.

Penton D, Czogalla J & Loffing J (2015). Dietary potassium and the renal control of salt balance and blood pressure. *Pflügers Arch Eur J Physiol* **467,** 513–530.

Piala AT, Moon TM, Akella R, He H, Cobb MH & Goldsmith EJ (2014). Chloride sensing by WNK1 involves inhibition of autophosphorylation. *Sci Signal* **7,** ra41.

Picard N, Trompf K, Yang C-L, Miller RL, Carrel M, Loffing-Cueni D, Fenton RA, Ellison DH & Loffing J (2014). Protein phosphatase 1 inhibitor-1 deficiency reduces phosphorylation of renal NaCl cotransporter and causes arterial hypotension. *J Am Soc Nephrol* **25,** 511–522.

Pohl M, Kaminski H, Castrop H, Bader M, Himmerkus N, Bleich M, Bachmann S & Theilig F (2010). Intrarenal renin angiotensin system revisited: Role of megalin-dependent endocytosis along the proximal nephron. *J Biol Chem* **285,** 41935–41946.

Rabinowitz L (1996). Aldosterone and potassium homeostasis. *Kidney Int* **49,** 1738–1742.

Reichold M, Zdebik AA, Lieberer E, Rapedius M, Schmidt K, Bandulik S, Sterner C, Tegtmeier I, Penton D, Baukrowitz T, Hulton S-A, Witzgall R, Ben-Zeev B, Howie AJ, Kleta R, Bockenhauer D & Warth R (2010). KCNJ10 gene mutations causing EAST syndrome (epilepsy, ataxia, sensorineural deafness, and tubulopathy) disrupt channel function. *Proc Natl Acad Sci U S A* **107,** 14490–14495.

Rengarajan S, Lee DH, Oh YT, Delpire E, Youn JH & McDonough A a (2014). Increasing plasma [K+] by intravenous potassium infusion reduces NCC phosphorylation and drives kaliuresis and natriuresis. *Am J Physiol Renal Physiol* **306,** F1059–F1068.

Richardson C, Rafiqi FH, Karlsson HKR, Moleleki N, Vandewalle A, Campbell DG, Morrice N a & Alessi DR (2008). Activation of the thiazide-sensitive Na+-Cl- cotransporter by the WNK-regulated kinases SPAK and OSR1. *J Cell Sci* **121,** 675–684.

Schweda F, Wagner C, Krämer BK, Schnermann J & Kurtz A (2003). Preserved macula densa-dependent renin secretion in A1 adenosine receptor knockout mice. *Am J Physiol Renal Physiol* **284,** F770–F777.

Simon DB, Nelson-Williams C, Bia MJ, Ellison D, Karet FE, Molina a M, Vaara I, Iwata F, Cushner HM, Koolen M, Gainza FJ, Gitleman HJ & Lifton RP (1996). Gitelman's variant of Bartter's syndrome, inherited hypokalaemic alkalosis, is caused by mutations in the thiazide-sensitive Na-Cl cotransporter. *Nat Genet* **12,** 24–30.

Sorensen M V, Grossmann S, Roesinger M, Gresko N, Todkar AP, Barmettler G, Ziegler U, Odermatt A, Loffing-Cueni D & Loffing J (2013). Rapid dephosphorylation of the renal sodium chloride cotransporter in response to oral potassium intake in mice. *Kidney Int* **83,** 811–824.

Terker AS, Yang C-L, McCormick J a, Meermeier NP, Rogers SL, Grossmann S, Trompf K, Delpire E, Loffing J & Ellison DH (2014). Sympathetic stimulation of thiazide-sensitive sodium chloride cotransport in the generation of salt-sensitive hypertension. *Hypertension* **64,** 178–184.

Terker AS, Zhang C, Erspamer KJ, Gamba G, Yang C-L & Ellison DH (2016). Unique chloride-sensing properties of WNK4 permit the distal nephron to modulate potassium homeostasis. *Kidney Int* **89,** 127–134.

Terker AS, Zhang C, McCormick J a, Lazelle R a, Zhang C, Meermeier NP, Siler D a, Park HJ, Fu Y, Cohen DM, Weinstein AM, Wang W-H, Yang C-L & Ellison DH (2015). Potassium Modulates Electrolyte Balance and Blood Pressure through Effects on Distal Cell Voltage and Chloride. *Cell Metab* **21,** 39–50.

Vallon V, Schroth J, Lang F, Kuhl D & Uchida S (2009). Expression and phosphorylation of the Na+-Cl- cotransporter NCC in vivo is regulated by dietary salt, potassium, and SGK1. *Am J Physiol Renal Physiol* **297,** F704–F712.

Vitzthum H, Seniuk A, Schulte LH, Müller ML, Hetz H & Ehmke H (2014). Functional coupling of renal K+ and Na+ handling causes high blood pressure in Na+ replete mice. *J Physiol* **592,** 1139–1157.

Wade JB, Liu J, Coleman R, Grimm PR, Delpire E & Welling PA (2015). SPAK-mediated NCC regulation in response to low-K+ diet. *Am J Physiol Renal Physiol* **308,** F923–F931.

Wagner C a, Loffing-Cueni D, Yan Q, Schulz N, Fakitsas P, Carrel M, Wang T, Verrey F, Geibel JP, Giebisch G, Hebert SC & Loffing J (2008). Mouse model of type II Bartter's syndrome. II. Altered expression of renal sodium- and water-transporting proteins. *Am J Physiol Renal Physiol* **294,** F1373–F1380.

Weinstein AM (2012). Potassium excretion during antinatriuresis: perspective from a distal nephron model. *Am J Physiol Renal Physiol* **302,** F658–F673.

Wilson FH, Disse-Nicodème S, Choate K a, Ishikawa K, Nelson-Williams C, Desitter I, Gunel M, Milford D V, Lipkin GW, Achard JM, Feely MP, Dussol B, Berland Y,

Unwin RJ, Mayan H, Simon DB, Farfel Z, Jeunemaitre X & Lifton RP (2001). Human hypertension caused by mutations in WNK kinases. *Science* **293,** 1107–1112.

Zhang C, Wang L, Zhang J, Su X-T, Lin D-H, Scholl UI, Giebisch G, Lifton RP & Wang W-H (2014). KCNJ10 determines the expression of the apical Na-Cl cotransporter (NCC) in the early distal convoluted tubule (DCT1). *Proc Natl Acad Sci U S A* **111,** 11864–11869.

Competing interests

The authors declare no competing interests

Author contributions:

The work for this study was carried out at University of Zurich, University of Regensburg, Christian-Albrecht University of Kiel, and University of Lausanne. DP designed and performed experiments (kidney slices preparation) analyzed and interpreted the data and contributed to manuscript writing. JC designed and performed experiments (Intravenous KCl injection, isolated perfused mouse kidney) analyzed and interpreted the data and contributed to manuscript writing. AW contributed data and performed data analysis. NH designed and performed the isolated DCTs experiment, analyzed and interpreted the data and contributed to manuscript writing. DLC designed and performed immunoblottings and analyzed the data. MC contributed data and performed data analysis, RDR contributed data and performed data analysis. OS contributed to the conception of the study and to writing the manuscript. MB contributed to the conception of the work, to the design of the DCT isolation experiments and to manuscript writing. FS contributed to the conception of the study, to the design and set up of the isolated perfused kidney technique and to writing the manuscript. JL conceived the study and contributed to the writing of the manuscript.

All authors approved the final version of the manuscript; agree to be accountable for all aspects of the work in ensuring that questions related to the accuracy or integrity of any part of the work are appropriately investigated and resolved. All persons designated as authors qualify for authorship, and all those who qualify for authorship are listed.

Financial support

David Penton is a fellow of the Program on Integrative Kidney Physiology and Pathophysiology (IKPP2) funded by the European Union's Seventh Framework Program for research, technological development and demonstration under grant agreement no 608847. NH and MB received support from the National Institutes of Health (NIH R01DK084059). Frank Schweda is supported by the German Research Foundation DFG (SFB699). Johannes Loffing and Olivier Staub are supported by research funds from the Swiss National Centre for Competence in Research "Kidney.CH", by project grants from the Swiss National Science Foundation (310030_143929/1 to JL and 310030_159765/1 to OS) and by the COST Action ADMIRE BM1301. JC, AW, MC, DLC, RDR are university staff members and did not received any external funding for this work.

Acknowledgments

The authors thank Prof. Richard Warth for fruitful discussions and gratefully acknowledge the technical assistance of Robert Götz and Michèle Heidemeyer. We also thank Prof. Vartan Kurtcuoglu for his help with the mathematical analysis of the data and Ms. Julia Graf for her contribution to the initial immunofluorescent characterization of the pNKCC2 antibody. We also thank Dr. Eilidh Craigie for careful proofreading of the manuscript. A setup for the isolated perfused kidney was kindly provided by Prof. Wolf-Georg Forssmann.

Titles and legends

Figure 1: Plasma [K^+] directly and rapidly controls NCC phosphorylation in the intact kidney *in vivo* and *ex vivo*. **A**, **B, C**, Changes in plasma K^+, Na^+ and aldosterone concentrations (respectively) 5 or 15 min after intravenous injection of 100 µl of vehicle (3 mice) or 80 mmol/L KCl in mice (4-5 mice per group). Dots represent independent measurements and bars represent the mean of each group. * $p<0.05$, ** $p<0.01$ compared to vehicle injection, using unpaired Student's t-test. **D**: Representative immunoblot (from mice in panels A,B,C) showing the changes in NCC phosphorylation in response to plasma [K^+] elevations. **E**: Representative immunoblot of isolated perfused mouse kidneys ("P") showing the modulation of NCC expression and phosphorylation at different phospho-sites upon changes in $[K^+]_{ex}$ ("C": non-perfused contralateral controls) **F:** Summary of 18 experiments showing the dependence of NCC phosphorylation on the $[K^+]_{ex}$. Each dot represents the ratio of NCC phosphorylation between the perfused kidney and the non-perfused contralateral kidney from one mouse. Dashed red line represents a sigmoidal fitting (see supplementary excel sheet for details). **G**: Immunofluorescence staining of pT53NCC (upper images) and the closely related cotransporter pNKCC2 phosphorylated in T96 and T101 (lower images) in kidneys perfused with 4.5 or 10 mmol/L $[K^+]_{ex}$. Scale bar: 250 µm.

Fig 2: *Ex vivo* kidney slice preparation recapitulates the findings in intact mice and isolated perfused kidney. **A**: Representative experiment showing the expression and phosphorylation of NCC at T53 in kidney slices incubated for 1h in control buffer (3 mmol/L $[K^+]_{ex}$). **B**: Summary of the expression and phosphorylation of NCC at T53 in kidney slices incubated under control conditions for 1h (n=19 slices, 10 mice). **C**: Representative western blot showing the expression and phosphorylation of NCC at position T53 under control (3 mmol/L) or high (10 mmol/L) $[K^+]_{ex}$ incubation conditions. Samples at t0 (after 30 min equilibration) were run in the same gel as the rest for every given antibody but not in sequential position. **D**: Summary of phosphorylation of NCC at position T53 in kidney slices incubated under control (3 mmol/L) or high (10 mmol/L) $[K^+]_{ex}$ conditions (n=8-17 slices, 3-7 mice). In the whole figure *** $p<0.001$ unpaired Student's t-test compared to control incubation. In panels B and D mean ± SEM is represented.

Figure 3: Regulation of NCC phosphorylation by maneuvers affecting DCT membrane voltage. **A**: Representative experiment showing the dose/response modulation of NCC phosphorylation by $[K^+]_{ex}$ at different phosphorylation sites in kidney slices. **B**: Expression of tNCC upon incubation with different $[K^+]_{ex}$ (n=6-7 slices per treatment, 2 mice). **C**: Changes in NCC phosphorylation at position T53 upon incubation with different $[K^+]_{ex}$ (n=8-17 slices per treatment, 3-7 mice). ** $p<0.01$, ***$p<0.001$ unpaired Student's t-test compared to control $[K^+]_{ex}$ (3 mmol/L). **D:** Representative experiment showing the reversibility of NCC dephosphorylation triggered by high $[K^+]_{ex}$. Control, high and low stand for 3, 10 and 1 mmol/L $[K^+]_{ex}$ respectively. This experiment was repeated 2 times (2 mice) with similar results**. E** and **F**: Effect of $BaCl_2$ (5 mmol/ L) on NCC phosphorylation (n=6 slices per treatment, 2 mice). **G:** Changes in NCC phosphorylation in hand isolated DCTs microperfused with 2 mmol/L $[K^+]_{ex}$ from the luminal side and either 1 or 10 mmol/L $[K^+]_{ex}$ from the basolateral side for 10 min. Each band represents a pool of 10 DCTs. In the whole figure ***$p<0.001$, ns non-significant using unpaired Student's t-test. In B, C and F, points represent individual experiments (slices) and bars represent the mean of the given treatment.

Figure 4: Effect of $[K^+]_{ex}$ on NCC and SPAK/OSR1 phosphorylation in native DCT cells is affected by changes in Cl^- conductances. **A**: Representative immunoblot showing the changes in tNCC and pT53NCC as well as SPAK and pSPAK-pOSR1 in kidney slices treated with low (1 mmol/L), control (3 mmol/L) or high (10 mmol/L) $[K^+]_{ex}$ under control (110 mmol/L) $[Cl^-]_{ex}$ conditions. **B**: Same experiment as in **A** but under 5 mmol/L $[Cl^-]_{ex}$. **C**: Summary of the effect of $[K^+]_{ex}$ on NCC phosphorylation at position T53 under control or low $[Cl^-]_{ex}$ (n=9-18 slices per treatment, 3-6 mice). **D**: Summary of the effect of $[K^+]_{ex}$ on SPAK/OSR1 phosphorylation at position T53 under control or low $[Cl^-]_{ex}$ (n=6 slices per treatment, 2 mice). In panels C and D * $p<0.05$, ** $p<0.01$, *** $p<0.001$, compared to the control condition ($[K^+]_{ex}$ 3 mmol/L) of each $[Cl^-]_{ex}$; & $p<0.05$ compared to the control condition of 110 mmol/L $[Cl^-]_{ex}$ using ANOVA with Bonferroni's multiple comparison post-test. **E**: Representative experiment showing the changes in NCC expression and phosphorylation at T53 in the presence or absence of the $[Cl^-]$ channel blocker DIDS upon treatment with control (3 mmol/L) or high (10 mmol/L) $[K^+]_{ex}$. **F**: Densitometric analysis of E (n=3 slices per treatment, 1 mouse). * $p<0.05$ compared to control of each condition using unpaired Student's t-test. **G**: Stimulation of NCC phosphorylation by isoproterenol (100 nmol/L) under low (5 mmol/L) $[Cl^-]_{ex}$.

Figure 5: Inhibition of protein phosphatases 1, 2A and 3 does not impair the dephosphorylation of NCC upon high $[K^+]_{ex}$. Representative western blot showing the changes in NCC expression and phosphorylation at position T53 in slices treated with control (3 mmol/L) or high (10 mmol/L) $[K^+]_{ex}$ under control (110 mmol/L) $[Cl^-]_{ex}$. **A**: Effect of inhibition of protein phosphatases 1 and 2A with calyculin A. **B:** Effect of inhibition of protein phosphatase 3 (calcineurine) with tacrolimus. **C:** Summary of the densitometric analysis of 6-12 slices per condition, 2-4 mice per experimental group.

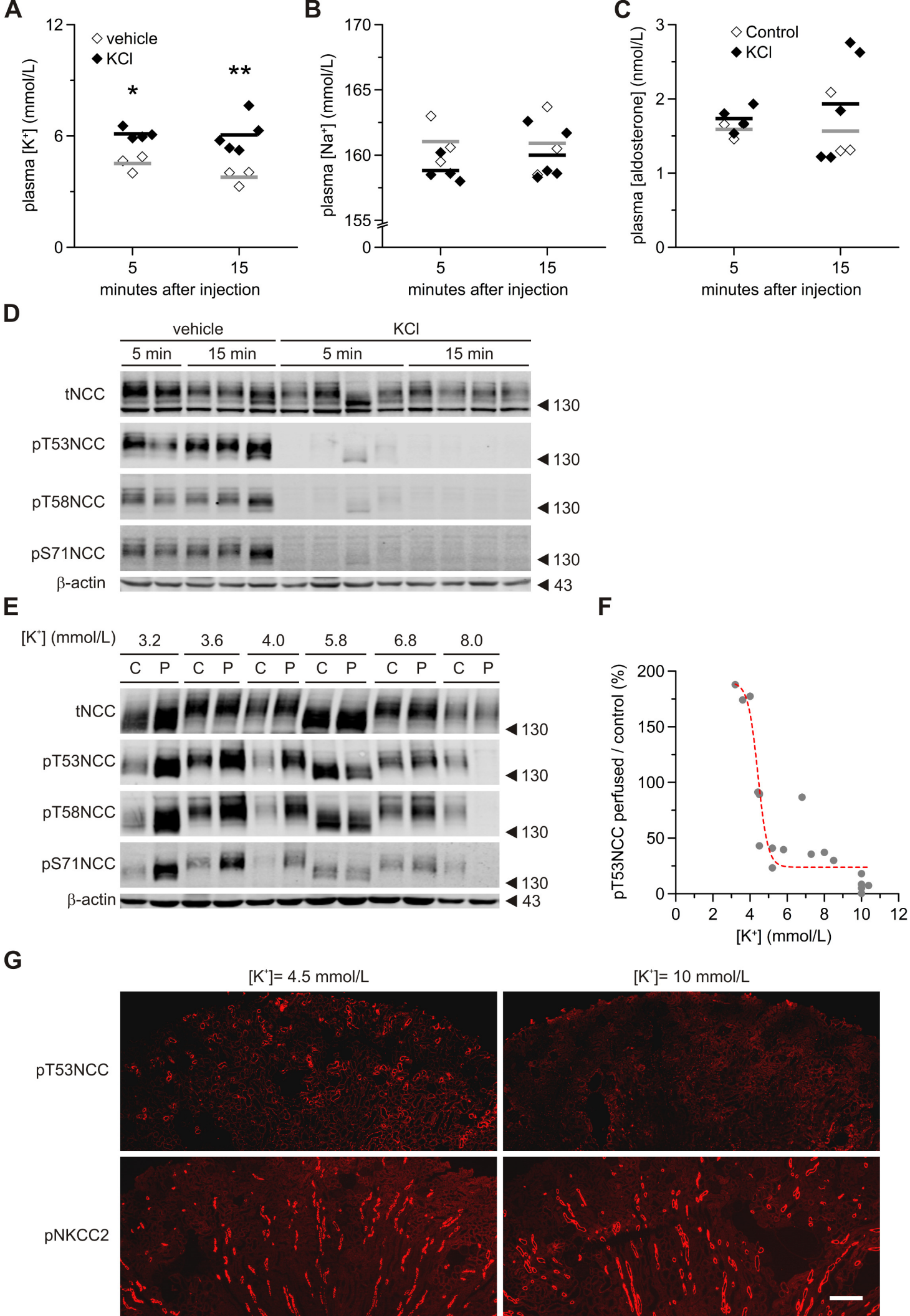
A
plasma [K+] (mmol/L)
vehicle
KCl
*
**
minutes after injection
B
plasma [Na+] (mmol/L)
minutes after injection
C
plasma [aldosterone] (nmol/L)
Control
KCl
minutes after injection
D
vehicle
KCl
5 min
15 min
5 min
15 min
tNCC
pT53NCC
pT58NCC
pS71NCC
β-actin
130
43
E
[K+] (mmol/L)
3.2
3.6
4.0
5.8
6.8
8.0
C P
tNCC
pT53NCC
pT58NCC
pS71NCC
β-actin
130
43
F
pT53NCC perfused / control (%)
[K+] (mmol/L)
G
[K+]= 4.5 mmol/L
[K+]= 10 mmol/L
pT53NCC
pNKCC2

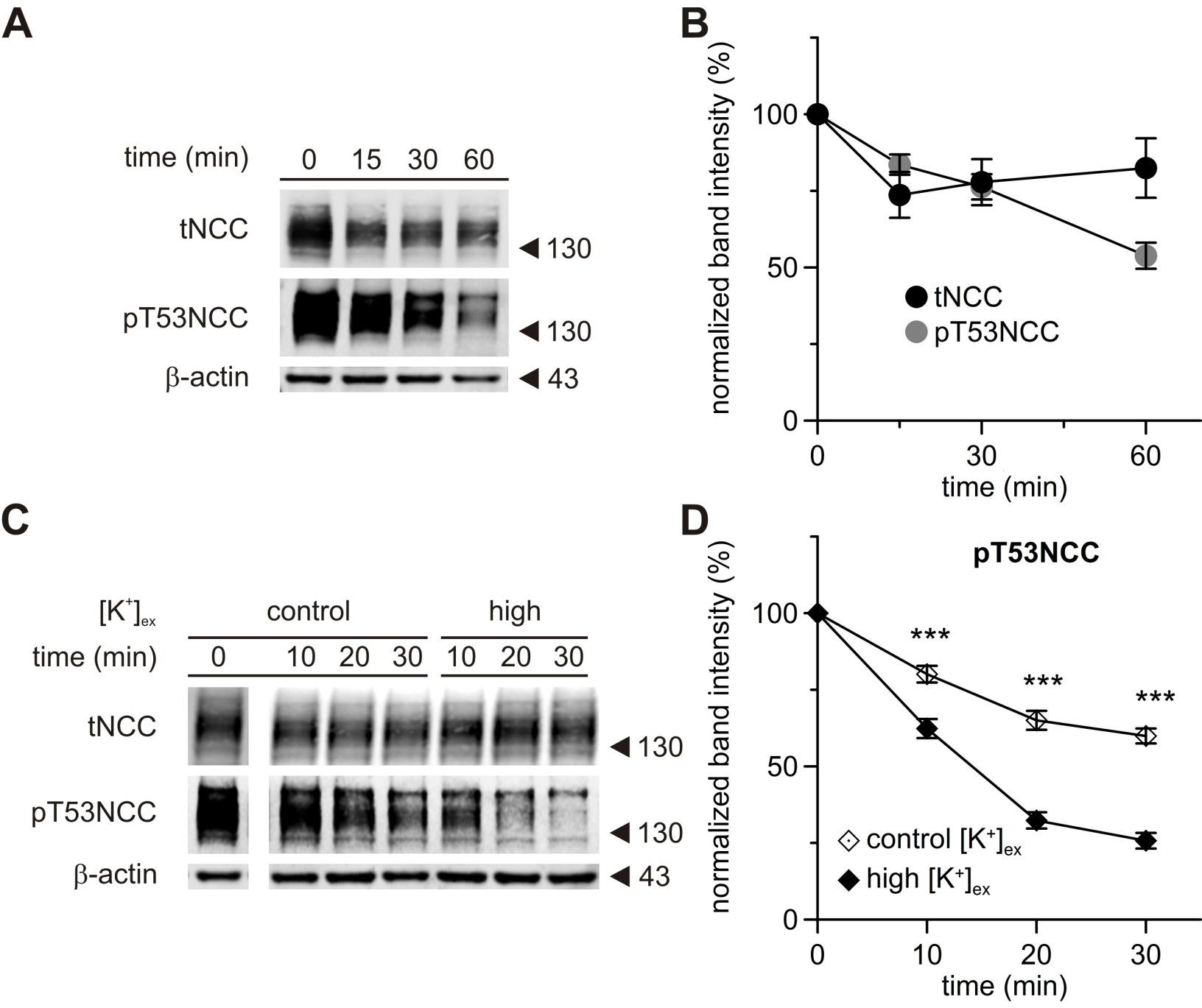
A
time (min)
0
15
30
60
tNCC
130
pT53NCC
130
β-actin
43
B
normalized band intensity (%)
100
50
0
tNCC
pT53NCC
0
30
60
time (min)
C
[K+]ex
control
high
time (min)
0
10
20
30
10
20
30
tNCC
130
pT53NCC
130
β-actin
43
D
pT53NCC
normalized band intensity (%)
100
50
0
***
***
***
control [K+]ex
high [K+]ex
0
10
20
30
time (min)

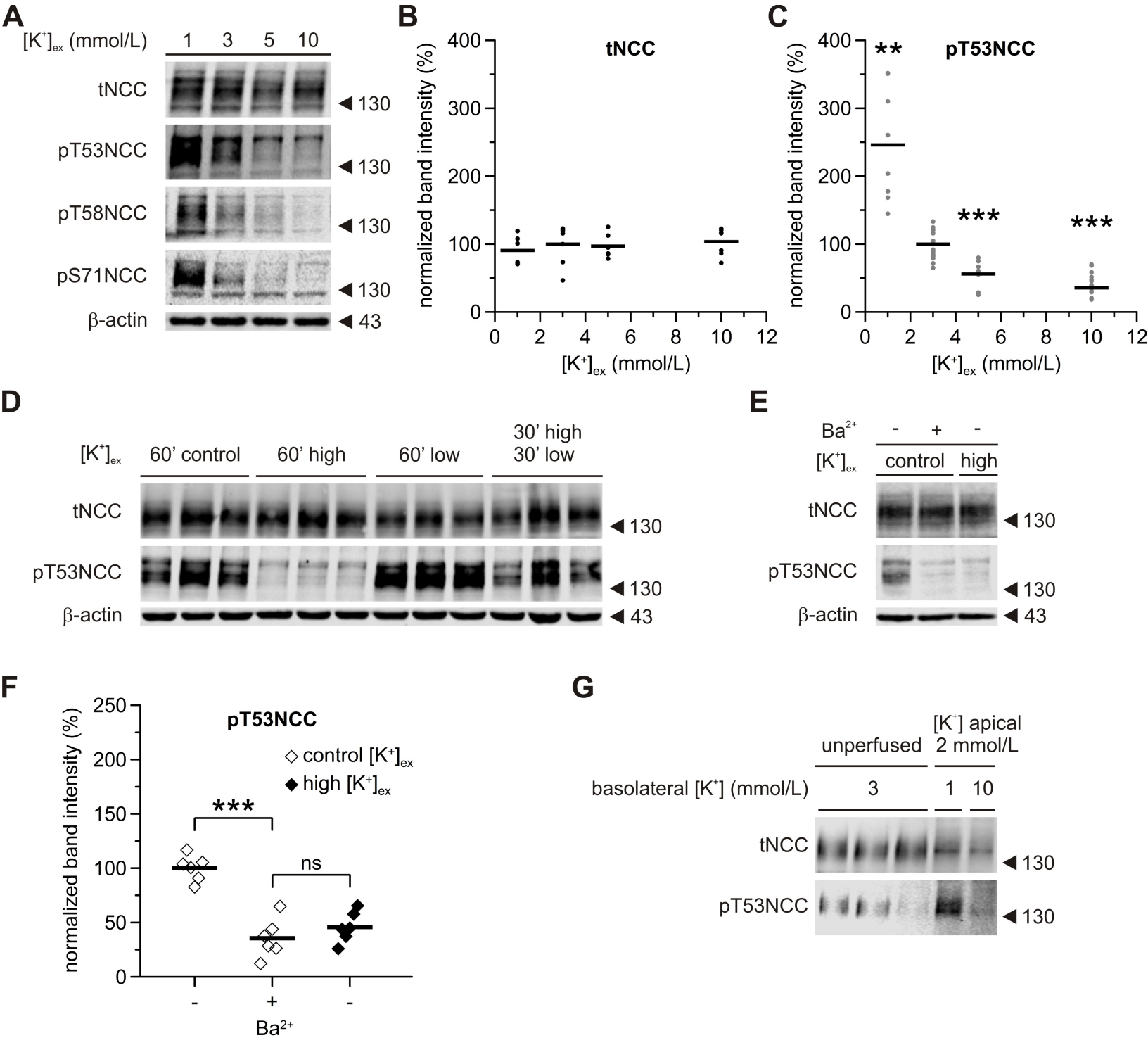
A
[K+]ex (mmol/L)
1
3
5
10
tNCC
pT53NCC
pT58NCC
pS71NCC
β-actin
130
130
130
130
43
B
tNCC
normalized band intensity (%)
400
300
200
100
0
0
2
4
6
8
10
12
[K+]ex (mmol/L)
C
pT53NCC
**
***
***
normalized band intensity (%)
400
300
200
100
0
0
2
4
6
8
10
12
[K+]ex (mmol/L)
D
[K+]ex
60' control
60' high
60' low
30' high
30' low
tNCC
pT53NCC
β-actin
130
130
43
E
Ba2+
-
+
-
[K+]ex
control
high
tNCC
pT53NCC
β-actin
130
130
43
F
pT53NCC
◇ control [K+]ex
◆ high [K+]ex
***
ns
normalized band intensity (%)
250
200
150
100
50
0
-
+
-
Ba2+
G
unperfused
[K+] apical
2 mmol/L
basolateral [K+] (mmol/L)
3
1
10
tNCC
pT53NCC
130
130

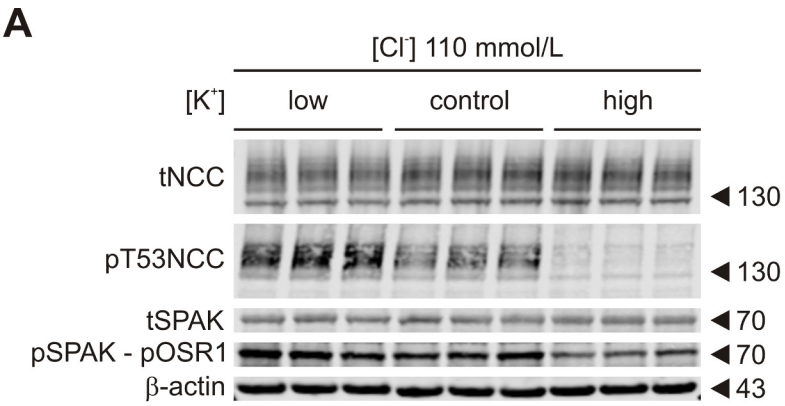
A
[Cl-] 110 mmol/L
[K+]
low
control
high
tNCC
pT53NCC
tSPAK
pSPAK - pOSR1
β-actin
130
130
70
70
43

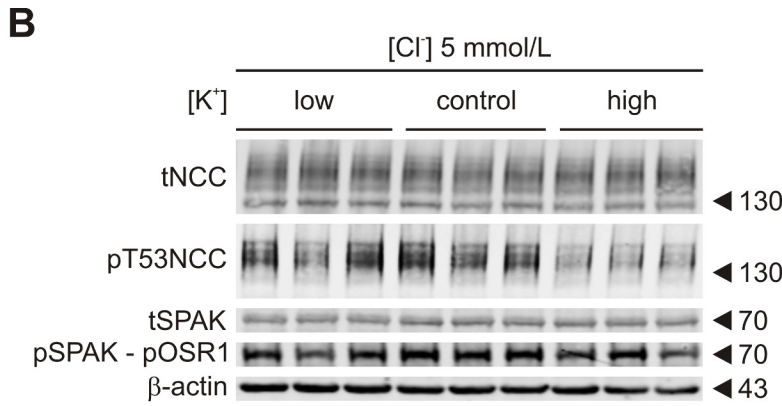
B
[Cl-] 5 mmol/L
[K+]
low
control
high
tNCC
pT53NCC
tSPAK
pSPAK - pOSR1
β-actin
130
130
70
70
43

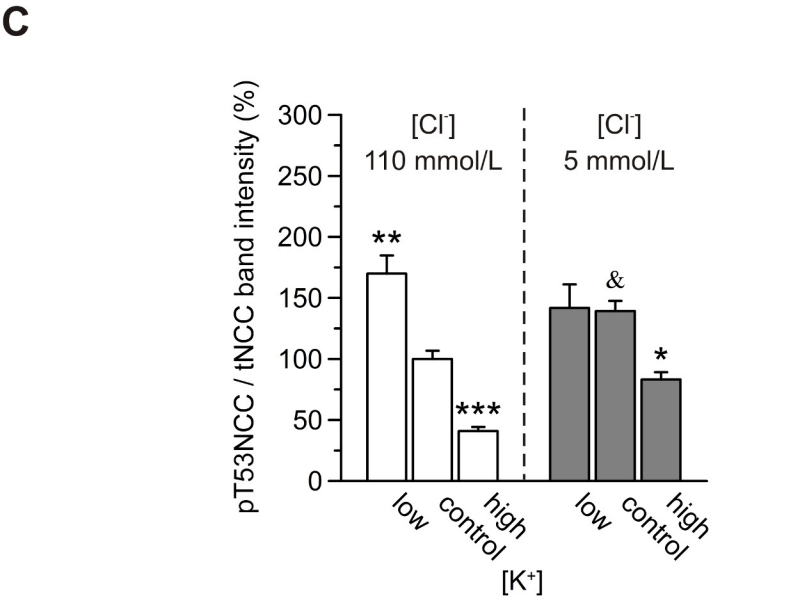
C
pT53NCC / tNCC band intensity (%)
300
250
200
150
100
50
0
[Cl-]
110 mmol/L
[Cl-]
5 mmol/L
**
***
&
*
low
control
high
low
control
high
[K+]

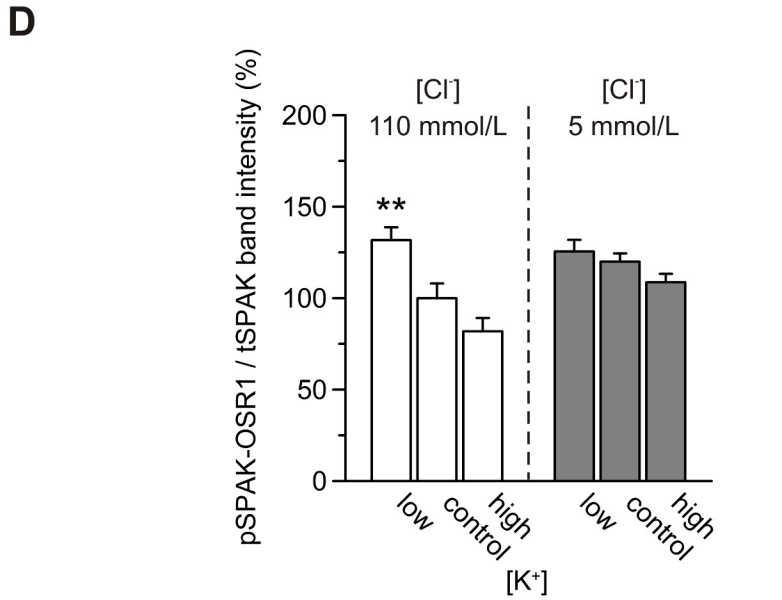
D
pSPAK-OSR1 / tSPAK band intensity (%)
200
150
100
50
0
[Cl-]
110 mmol/L
[Cl-]
5 mmol/L
**
low
control
high
low
control
high
[K+]

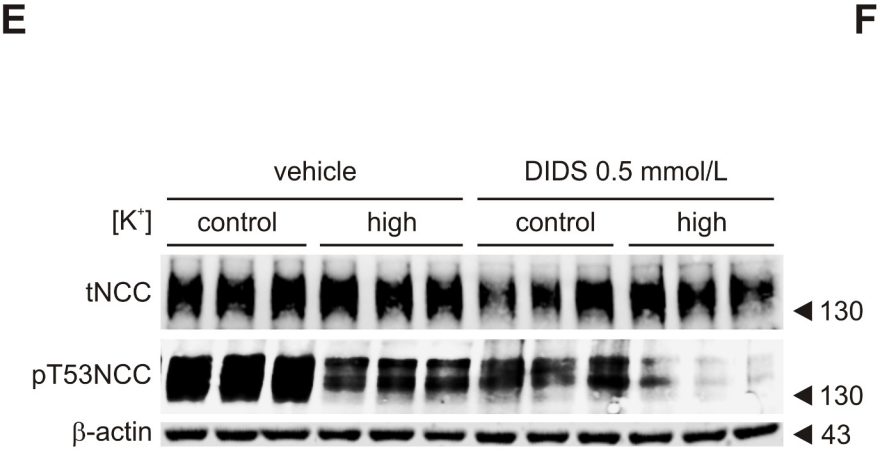
E
vehicle
DIDS 0.5 mmol/L
[K+]
control
high
control
high
tNCC
pT53NCC
β-actin
130
130
43

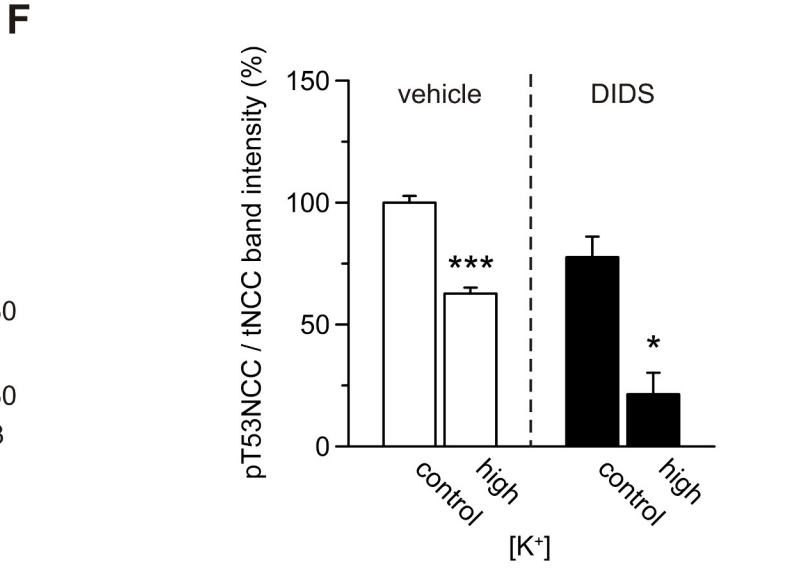
F
pT53NCC / tNCC band intensity (%)
150
100
50
0
vehicle
DIDS
***
*
control
high
control
high
[K+]

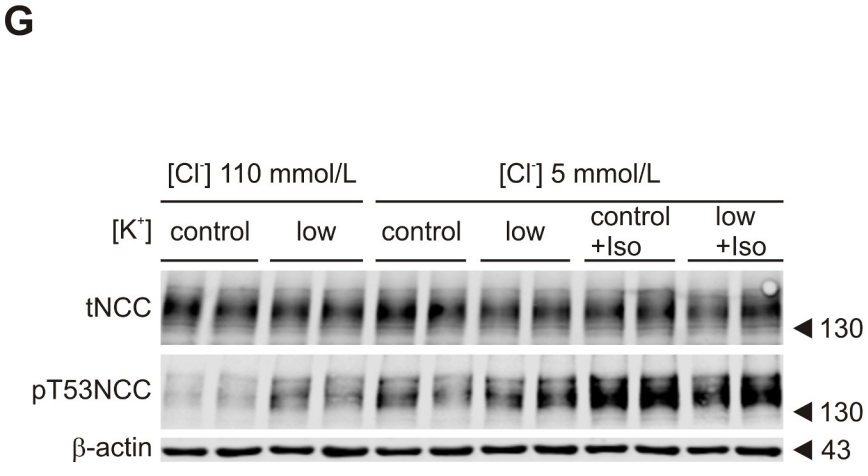
G
[Cl-] 110 mmol/L
[Cl-] 5 mmol/L
[K+]
control
low
control
low
control +Iso
low +Iso
tNCC
pT53NCC
β-actin
130
130
43

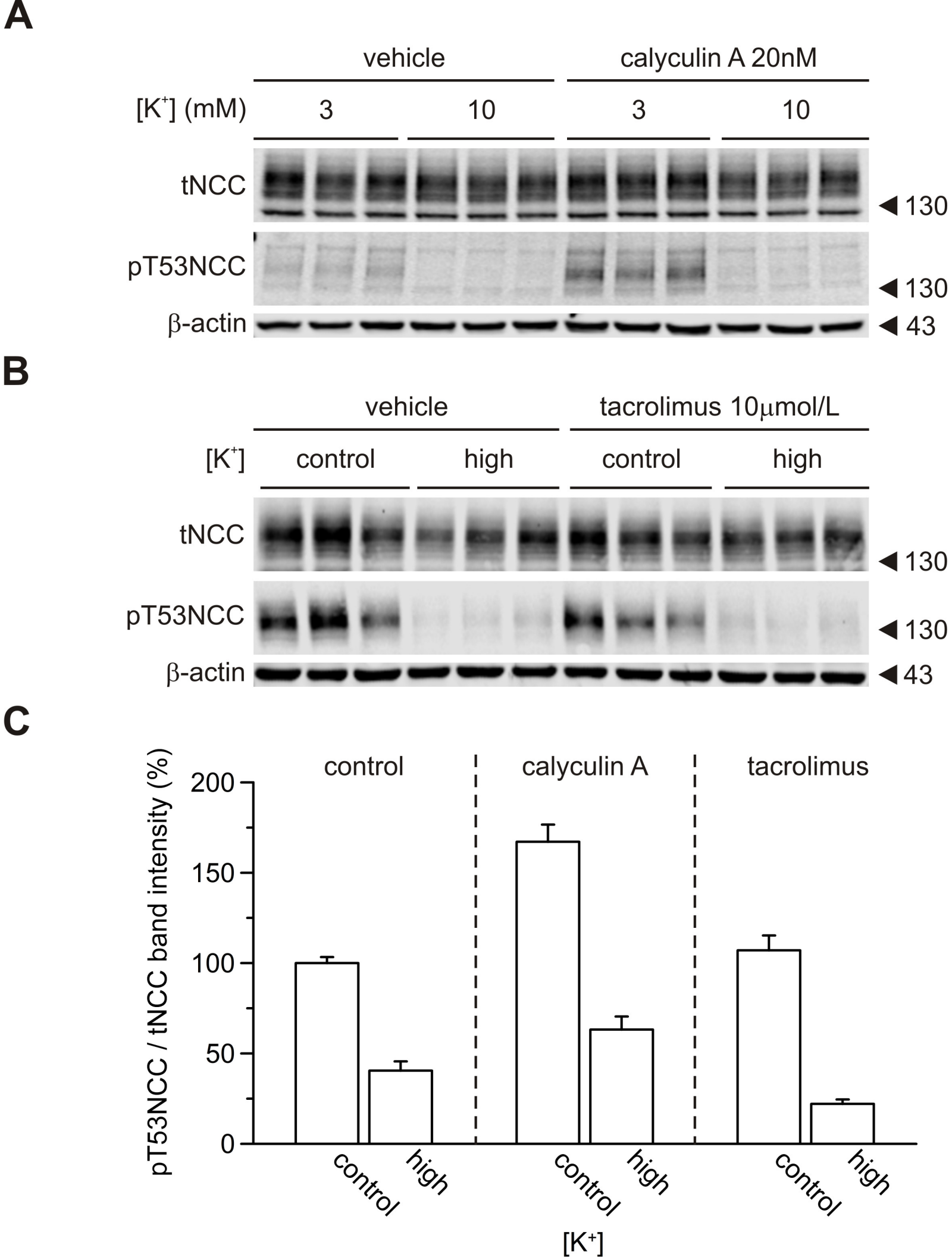
A
vehicle
calyculin A 20nM
[K+] (mM)
3
10
3
10
tNCC
130
pT53NCC
130
β-actin
43
B
vehicle
tacrolimus 10μmol/L
[K+]
control
high
control
high
tNCC
130
pT53NCC
130
β-actin
43
C
control
calyculin A
tacrolimus
pT53NCC / tNCC band intensity (%)
200
150
100
50
0
control
high
control
high
control
high
[K+]